Colloid and Interface Science Communications 36 (2020) 100261

Contents lists available at ScienceDirect

Colloid and Interface Science Communications

journal homepage: www.elsevier.com/locate/colcom

Collapse of Langmuir monolayer formed by the mixture of short- and long-tailed fatty acid molecules

Bijay K. Sah, Sarathi Kundu*

Soft Nano Laboratory, Physical Sciences Division, Institute of Advanced Study in Science and Technology, Vigyan Path, Paschim Boragaon, Garchuk, Guwahati, Assam 781035, India

ARTICLE INFO

Keywords:
Fatty acids
Mixed monolayer
Monolayer collapse
Out-of-plane structures
Structural modification

ABSTRACT

Surface pressure versus molecular area (π-*A*) isotherms of stearic acid (SA), behenic acid (BA) and their mixtures are studied at high subphase pH ($\approx$ 9.5) in presence of Ba^{2+} ions. It is found that the collapse pressure (π_C) and dip pressure (π_D) points of binary fatty acid monolayer varies depending on the relative amount of the two components and nearly follow the Langmuir growth model. Out-of-plane structures obtained from the X-ray reflectivity and atomic force microscopy analysis imply that SA shows multi-layered structure that gradually decreases with the decrease in SA proportion in the mixed film. The transition from constant pressure to constant area collapse is observed when the weightage of BA becomes $\geq$66% for the mixed film. The change in the collapse behaviour and collapsed structure is explained using the two-dimensional percolated networks formed by the tail-tail hydrophobic interactions of relatively more hydrophobic long-chained BA molecules.

1. Introduction

Langmuir monolayers of lipids and fatty acids can be considered as a two-dimensional model system at air-water interface with the ability to investigate the nanoscale molecular interactions [1]. Langmuir monolayers are suitable to study different phenomena related to membrane behaviors [2–4], phase transitions [5], molecular recognitions [6–8], fluid dynamics [9], thermodynamics [10], etc. Furthermore, the films can be examined under different film and subphase conditions such as composition, packing density, temperature, pH, dissolved ions, etc. [11]. Depending on the amphiphiles, properties of the monolayer at interfaces are of keen interest in the fields of materials and biology [12–15]. The compression of such monolayers leads to phase transitions through different phases like gaseous, liquid expanded, liquid condensed, solid, etc. Under further compression the 2D nature of the monolayer is destabilised forming 3D structures; this is often referred as collapse [16]. Different models exist in literature to explain the collapse phenomenon. Reis model states that the monolayer collapse occurs through four steps, namely weakening, folding, bending and finally breaking [17]. Moreover, folding of monolayers into subphase, buckling, formation of islands and 3D grains, etc., are also proposed by different groups [18,19]. In general, monolayer collapse is an irreversible process, however reversible monolayer collapse is also seen for certain mixed monolayers such as lung surfactants where the surface tension regulates the functioning of the lung [20,21]. Understanding these 2D-3D transformations gives a better insight into the origin and formation of 3D ordered structures, e.g., twisted ribbons, giant folds and vesicles. Also the formation mechanism of defects in thin film, e.g., biological and optical coating fibres to protect the ears and the eyes, as well as the defects present in the inner lining of the human lungs can be elucidated [22]. A number of techniques are developed to visualize and characterize the collapsed monolayers, e.g., fluorescence microscopy, Brewster angle microscopy [23], X-ray reflectivity [24], atomic force microscopy [16], etc.

In general, there are two types of collapse behaviors observed by the shape of the π–*A* isotherms, in one case pressure falls suddenly after π_C, whereas in the other case it remains nearly constant after π_C. The former is known as 'constant area collapse' while the latter is known as 'constant pressure collapse' [25] .The physiochemical conditions and the nature of the constituent molecules mostly dictate the type of collapse occurring under over compression. Before the collapse pressure π_C, fatty acid molecules shows asymmetric configuration [25–28] with all their hydrophobic tails in the air side whereas the hydrophilic head groups are attached with the water of the air-water interface. Conventionally, such layers are referred to as asymmetric monolayer. After π_C, the film can take two different configurations; one shows a trilayer like structure while the other shows a multilayer structure. In the trilayer like structure, one symmetric monolayer (i.e., the tails exist on

* Corresponding author.
E-mail address: sarathi.kundu@gmail.com (S. Kundu).

https://doi.org/10.1016/j.colcom.2020.100261
Received 29 January 2020; Received in revised form 24 March 2020; Accepted 31 March 2020

both side of the headgroups) is formed above the asymmetric monolayer [25–27]. The symmetric monolayer is often considered as a bilayer where the tails are facing away from one another [29]. So the film is treated as a trilayer (summation of monolayer and a bilayer) structure. In multilayers, more than one bilayer or symmetric monolayer structure is formed above the monolayer. Generally, trilayer-like structure is observed for "constant pressure collapse" [25,27], whereas for the "constant area collapse" multilayer structure is formed [25]. For pure water or in the presence of Pb or Cd ions, fatty acids monolayer shows constant area collapse [30,31] and constant pressure collapse is observed in fatty acids monolayer at high pH condition in the presence of ions such as Zn, Mg, Co and Mn [25,27]. Generally, coexistence between trilayer and monolayer is seen in case of constant pressure collapse [27]. The main distinction between the two types of collapse arises due to cations-headgroup interaction and cations-cations interaction [25]. Though many studies exist on monolayer growth [27,32], morphology [23,33,34] and structure [27,35,36] during collapse but it is not well understood that why for some cations constant area collapse occurs while for other cations constant pressure collapse is observed. It should be noted that under certain conditions the presence of divalent ions in water also forms two-dimensional super lattices beneath the head groups of the fatty acid molecules [37].

Although monolayer collapse generally occurs at higher surface pressure ($\pi_C \approx 50$ mN/m) but reports on collapse at lower surface pressure also exist. Langmuir monolayer of DPPC (1,2-dipalmitoyl-sn-glycero-3 phosphocholine) molecule in presence of butylparabens shows monolayer collapse at lower surface pressure ($\pi_C \approx 28$ mN/m) [38]. Similarly, stearic acid monolayer in presence of barium ions at high pH conditions show monolayer to trilayer collapse even at lower surface pressure of ≈ 0.6 mN/m. The reason for such monolayer to multilayer transformation is due to the formation of bidentate chelate coordination [39]. In Langmuir monolayers the metal headgroup coordination occurs in three different ways: bidentate chelate coordination, bidentate bridging and unidentate coordination [40]. However, at lower pH, the metal headgroup coordination is unidentate but for higher pH condition the headgroup coordination gets modified into bidentate bridging, bidentate chelate, or both [41,42]. Although a number of studies are done on structural and morphological modifications, growth and mechanism of monolayer collapses, but a deeper understanding on monolayer collapse depending on different physiochemical conditions is still incomplete. The principles of 2D lattice percolation model [43–45] can be used to explain the monolayer collapse as fatty acid arrange themselves in a 2D lattice at the air-water interface with their headgroups forming different bonding configurations. Gopal and Lee have also used the concept of lattice percolation phenomenon in order to explain the collapse in mixed lipid monolayer system [46]. Usually percolation theory primarily deals with the system where the lattices are connected through pathways and their sites (or bonds) are occupied to different extents. The percolation threshold for 2D lattice is defined as the ratio of occupied sites (or bonds) connected through nearest neighbours over entire lattice. The concepts of percolation theory are used in different areas of research such as physics, geophysics, biology, engineering, etc.

In this article we have studied the collapse behaviour of a mixed monolayer composed of two different surfactants with the same head group but different chain length in presence of divalent ions (Ba^{2+}). The components chosen for the mixed Langmuir monolayer are stearic acid (SA) or octadecanoic acid ($C_{18}H_{36}O_2$) and behenic acid (BA) or docosanoic acid ($C_{22}H_{44}O_2$). The estimated tail lengths of the SA and BA are 2.5 and 2.9 nm respectively [29]. The mixed fatty acid (SA:BA) films are deposited before and after collapse on hydrophilic Si (001) substrate using modified version of the inverted Langmuir-Schaefer (MILS) technique [25,47]. The surface morphology of all the deposited films are studied through atomic force microscopy (AFM) and the out-of-plane structures are studied using x-ray reflectivity (XRR).

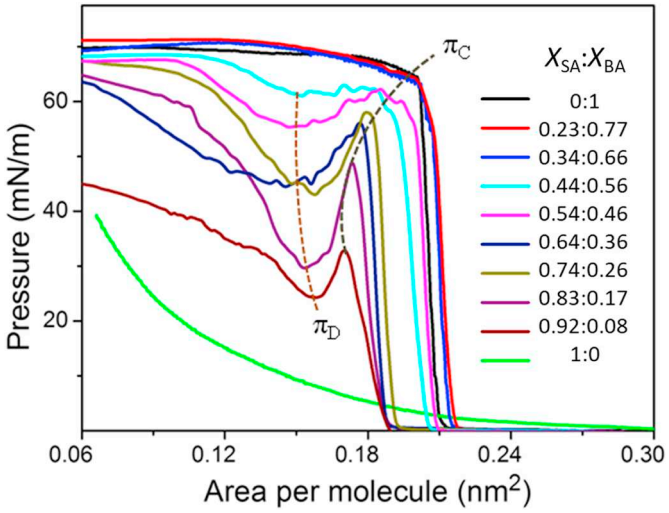

Fig. 1. Surface pressure - area per molecule (π - A) isotherms of SA and BA mixed langmuir monolayers in presence of Ba^{2+} ions at high subphase pH condition (≈ 9.5). Ten colours represent ten different mole fractions (X_{SA}: X_{BA}) of stearic and behenic acids as green (1.0:0.0), wine (0.92:0.08), purple (0.83:0.17), dark yellow (0.74:0.26), navy (0.64:0.36), magenta (0.54:0.46), cyan (0.44:0.56), blue (0.34:0.66), red (0.23:0.77) and black (0.0:1.0). The corresponding volume ratios of SA:BA films are: green (10:0), wine (9:1), purple (8:2), dark yellow (7:3), navy (6:4), magenta (5:5), cyan (4:6), blue (3:7), red (2:8) and black (0:10) respectively. (For interpretation of the references to colour in this figure legend, the reader is referred to the web version of this article.)

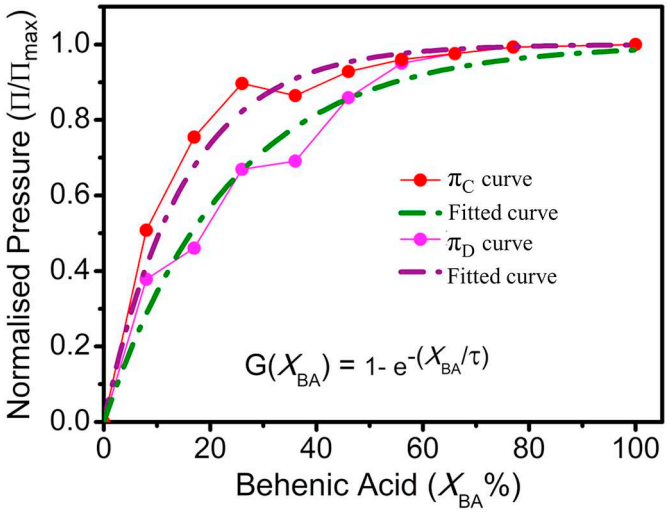

Fig. 2. Variation of collapse point (π_C) and dip pressure point (π_D) of pure SA, BA and mixed SA:BA monolayer with the increasing percentage of behenic acid in terms of mole fraction. The dash-dot lines are the corresponding exponential fit (Langmuir-like growth).

2. Experimental details

Stearic acid [$CH_3(CH_2)_{16}COOH$, Sigma, 99%] and behenic acid [$CH_3(CH_2)_{20}COOH$, Sigma, 99%] molecules were spread from a 1 mg/ml chloroform (Sigma, 99%) solution on Milli-Q water (resistivity 18.2 MΩ cm) containing barium chloride ($BaCl_2 \cdot 2H_2O$, Merck, 99%) in a Langmuir trough (Apex Instruments). The concentration of the barium salt was kept at ≈ 0.5 mM and the pH of the subphase was maintained at ≈ 9.5 for all the isotherm measurements and film depositions. To minimize the impurity no buffer was used to maintain the pH of the subphase. The mixed SA:BA monolayer composed of two fatty acids

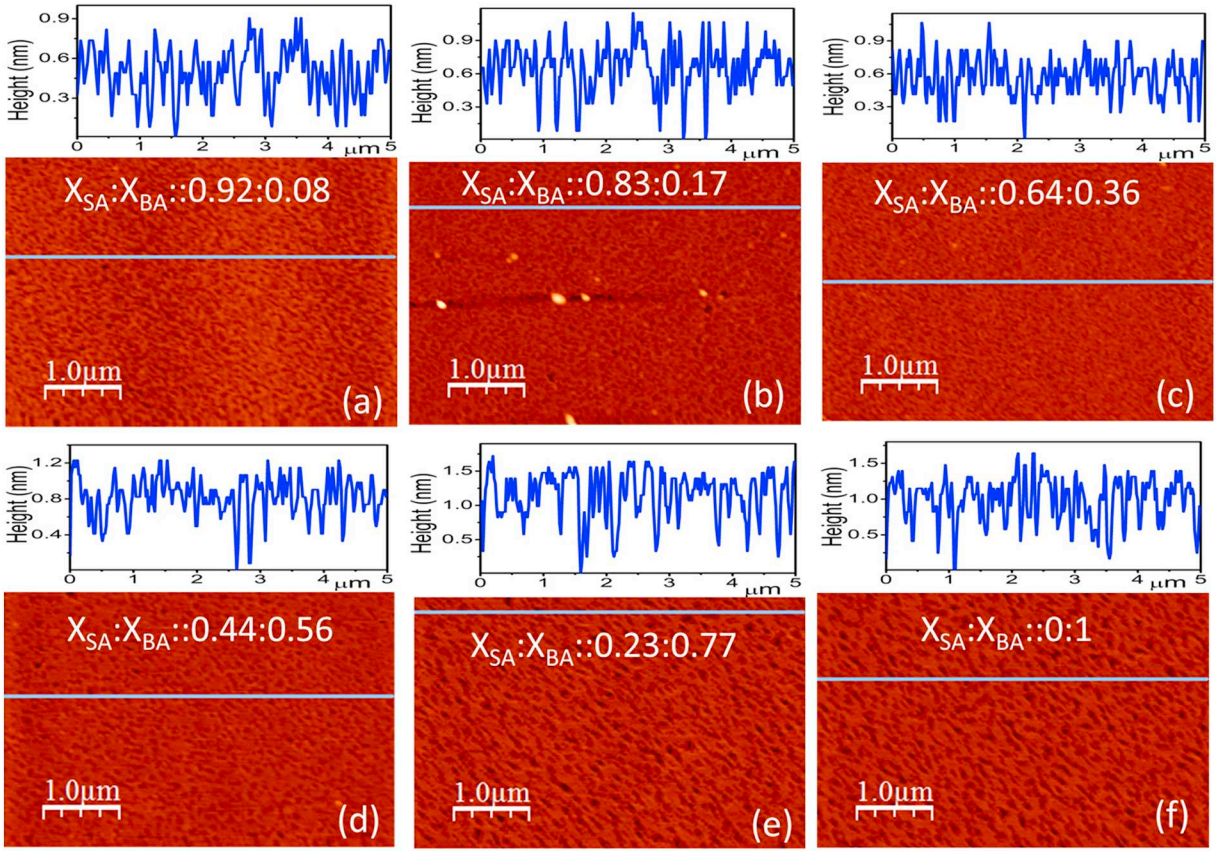

Fig. 3. AFM images of mixed SA:BA and pure BA films before the collapse pressure (π_C) in presence of Ba^{2+} ions at high subphase pH ($\approx$ 9.5) for different X_{SA}: X_{BA} ratios: (a) 0.92:0.08, (b) 0.83:0.17, (c) 0.64:0.36, (d) 0.44:0.56, (e) 0.23:0.77and (f) 0.0:1.0.

(stearic and behenic acid) was prepared just by mixing both the components in the same solvent (chloroform) prior to the spreading of the molecules at air-water interface. The trough is equipped with a Wilhelmy plate for surface pressure measurements and a pair of identical movable barrier for compression of the monolayers. The monolayer was compressed at a constant rate of 5 mm / min during all the isotherm measurements at room temperature ($\approx$ 24 °C). All the depositions were done by MILS method in a single up stroke. All the films were deposited at the depositing speed of 1.5 mm/min. Prior to the depositions, the Si (001) substrate are made hydrophilic by boiling them in a mixed solution of ammonium hydroxide (NH_4OH, Merck, 30%), hydrogen peroxide (H_2O_2, Merck, 30%), and Milli-Q water (H_2O: NH_4OH: H_2O_2 = 2: 1: 1, by volume) for 5–10 min at 100 °C. All the substrates are kept inside the Milli-Q water until MILS deposition. In MILS method, hydrophilic silicon substrate was kept horizontally on an L-shaped Teflon substrate holder attached to the clip of the trough dipper. The L-shaped substrate holder can be taken out from water to air side with a desired speed. In this deposition method, at first the water surface was properly cleaned and then the L-shaped substrate holder was immersed into water (containing barium chloride) so that the silicon substrate was kept parallel to and nearly 10 mm below the air-water interface. Pure and mixed SA and BA molecules were then spread on the water surface with the same amount and concentration as was spread at the time of isotherm measurements. Depositions were done before and after the collapse pressure (π_C). Before collapse, all films are deposited at 25 mN/m except pure SA as for that collapse occurred at very lower surface pressure ($\approx$ 0.6 mN/m).

Reflectivity studies of the SA:BA films were carried out using a X-ray diffractometer (XRD) setup. The diffractometer (D8 Advanced, Bruker AXS) has a Cu source (sealed tube) followed by a Göbel mirror to select and enhance Cu K_α radiation (λ = 1.54 Å). The scattered beams are detected using NaI scintillation (point) detector. All the data's are taken in the specular condition, i.e., both the incident angle (θ) and the reflected angle (θ) are equal and lie in the same scattering plane. In such specular condition, the momentum transfer vector has only one non vanishing component, q_z, normal to the surface which is given by $q_z = (4\pi/\lambda) \sin\theta$. The analysis of XRR data is done using Parratt's formalism [48] where the film is assumed to be a stack of a number of homogeneous layers with sharp interfaces. The surface and interfacial roughness is included during the analysis of the XRR data [49,50]. An electron density profile (EDP) is extracted from the fit which gives the average electron density (ρ) as a function of depth (z) with high resolution [49–51]. Details of models used for fitting the reflectivity data are described in supporting information. The surface topography of all the deposited films are studied using NTEGRA Prima, NT-MDT Technology, atomic force microscope (AFM) having silicon cantilever with a spring constant of $\approx$ 11.8 N/m. All the scans were carried out in semi-contact mode. The scan size for all samples was 5 μm × 5 μm. Scans were performed several times at a scan rate of 1 Hz over different region of the film. Image processing and analysis of the AFM images were done by the WSxM software [52].

3. Results and discussion

The surface pressure – area per molecule (π - A) isotherm for pure SA, BA and the mixed SA:BA monolayer at different volume ratios in presence of Ba^{2+} ions are demonstrated in Fig. 1. The pH of the subphase for all the isotherms is maintained at $\approx$ 9.5. Pure stearic acid and behenic acid isotherms curves are shown by the red and black curves respectively.

Different volume ratios of SA:BA are distinguished using different colour codes: wine (9:1), purple (8:2), dark yellow (7:3), navy (6:4),

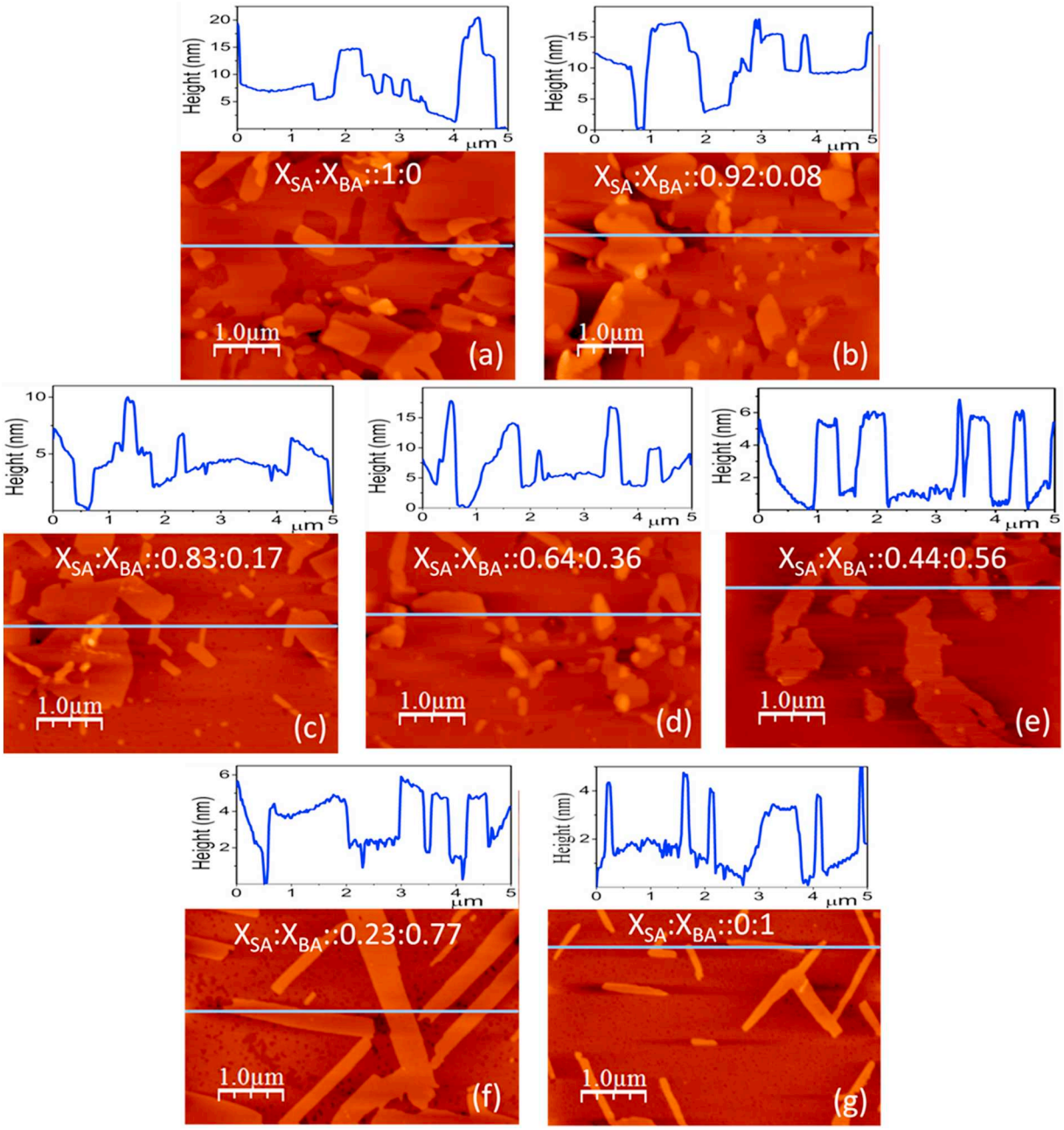

Fig. 4. AFM images of pure SA, BA and mixed SA:BA films after the collapse pressure (π_C) in presence of Ba^{2+} ions at high subphase pH ($\approx$ 9.5) for different X_{SA}: X_{BA} ratios: (a) 1.0:0.0 (b) 0.92:0.08, (c) 0.83:0.17, (d) 0.64:0.36, (e) 0.44:0.56, (f) 0.23:0.77 and (g) 0.0:1.0.

magenta (5:5), cyan (4:6), blue (3:7) and green (2:8). However, in terms of mole fraction, the ratios of stearic and behenic acids (X_{SA}: X_{BA}) are wine (0.92:0.08), purple (0.83:0.17), dark yellow (0.74:0.26), navy (0.64:0.36), magenta (0.54:0.46), cyan (0.44:0.56), blue (0.34:0.66) and green (0.23:0.77). At lower pH conditions fatty acid monolayer shows different phases which are identified by the changes in slope of the $\pi - A$ isotherm [53], X ray diffraction [1] and Brewster angle microscope [54]. Unlike at lower pH conditions, fatty acid at higher pH ($\approx$ 9.5) values do not show any tilted to untilted phase transition in the presence of Ba^{2+} ions [55]. The lift-off area (A_0) value for the BA isotherm is $\approx$ 0.22 nm^2. But the isotherm for SA does not show any specific A_0 value as the rise is gradual over a wide range of A value. However, the area per molecule starts to take non-zero value nearly at 0.30 nm^2. The mixed monolayers SA:BA isotherm curves are located in between the isotherm curves of pure fatty acids. For the mixed monolayers SA:BA, the values of A_0 varies from 0.19 nm^2 to 0.21 nm^2. The decrease in SA ratio or the increase in BA ratio in the mixed SA:BA film leads to the increase in A_0 value. Probably due to the reorganization of SA molecules from monolayer to layered structure, the A_0 value decreases with increasing the SA amount in the mixed film which is explained in the subsequent sections. The isothermal compressibility values [56] of the films obtained from the steep region of the isotherms are found between 0.0005 and 0.001 m/mN, however, the values take one or two orders of magnitude higher for the collapsed regions. Pure BA monolayer shows constant pressure collapses at the surface pressure (π_C) of $\approx$ 64.6 mN/m. But in case of pure SA monolayer the isotherm nature totally changes, the rise in pressure becomes relatively slower compared to the other isotherm curves. The film could attain a maximum pressure of about 39 mN/m having the area per molecule value as low as 0.06 nm^2. It thus strongly indicates that the SA film undergoes 2D-3D transition; moreover, this type of collapse may start at the very low surface pressure. For the mixed SA:BA monolayers the value of π_C

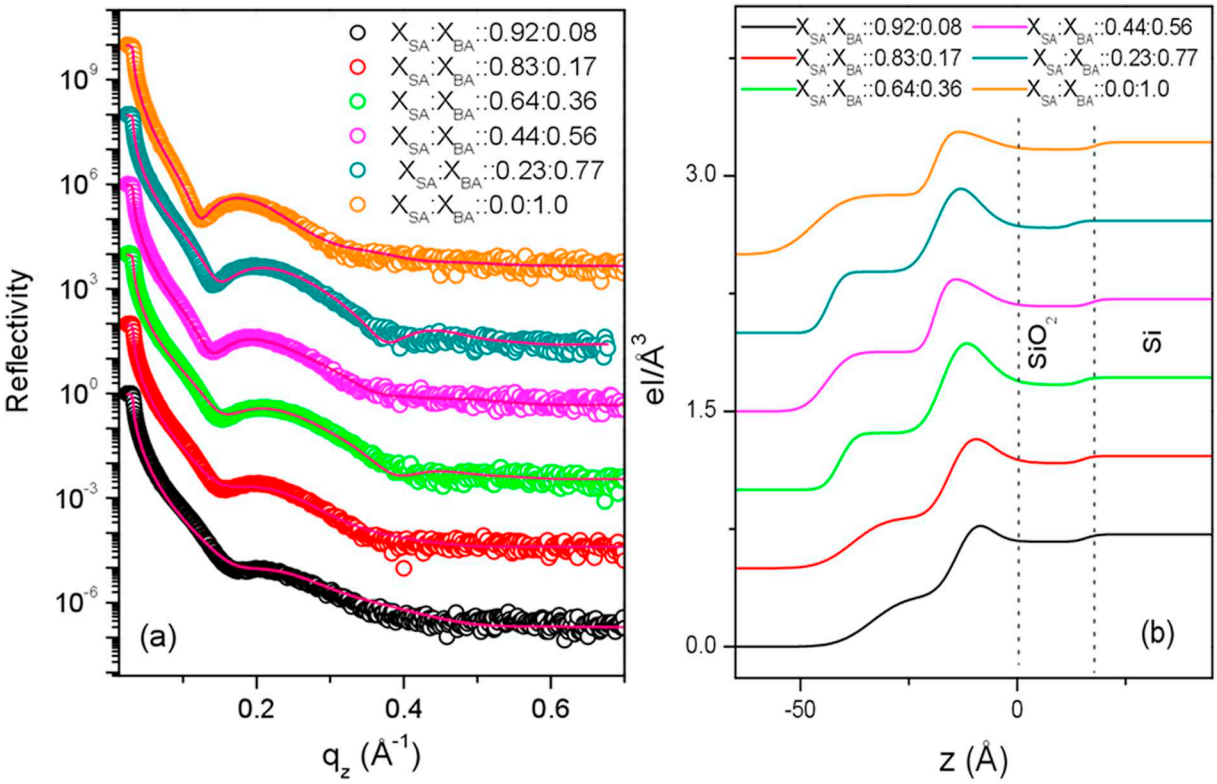

Fig. 5. (a) X-ray reflectivity data (open circles) and the respective fits (solid lines) for the films deposited before the collapse pressure (π_C) at six different ratios of SA:BA mixed films in presence of Ba^{2+} ions at high ($\approx$ 9.5) subphase pH condition. Reflectivity data and the corresponding fits have been vertically shifted for clarity. (b) Electron density profiles (EDPs) extracted from the fits is also shifted vertically for the same.

decreases gradually with the decrease in the BA proportion in the monolayer.

The values of π_C with changing X_{SA}: X_{BA} ratios in the mixed monolayer are obtained as follows: 32.8 mN/m (0.92:0.08), 48.8 mN/m (0.83:0.17), 57.9 mN/m (0.74:0.26), 55.9 mN/m (0.64:0.36), 60.0 mN/m (0.54:0.46), 62.0 mN/m (0.44:0.56), 63.0 mN/m (0.34:0.66) and 64.2 mN/m (0.23:0.77) respectively. In addition to that, mixed monolayer shows both type of collapse behaviour, i.e., constant pressure collapse and constant area collapse depending on the ratio of the individual component. Starting from pure behenic acid monolayer to mixed monolayer having BA weightage up to 66% shows constant pressure collapse behaviour. On the other hand, mixed monolayer having BA nearly in the range of 10% to 66% shows constant area collapse behaviour. For such films after collapse the surface pressure decreases up to a certain down or lower pressure point (π_D) and then the pressure starts to rise again on further compression. The corresponding values of π_D for different X_{SA}: X_{BA} ratios in the mixed monolayers are 61.4 mN/m (0.44:0.56), 55.5 mN/m (0.54:0.46), 44.6 mN/m (0.64:0.36), 43.2 mN/m (0.74:0.26), 29.7 mN/m (0.83:0.17) and 24.4 mN/m (0.92:0.08) respectively. The π_D value increases with the increasing amount of BA in the SA:BA monolayer. Fig. 2 shows the plot of π_D and π_C vs behenic acid ratio in the mixed SA:BA film. Both the curve clearly shows that the increase in π_C and π_D value with increasing BA ratio follows the Langmuir-like growth behaviour and it is expressed as $G(X_{SA}) = 1 - \exp.(-X_{SA}/\tau)$, where τ is the growth constant in terms of mole fraction. With the increase of BA amount or X_{BA} in the mixed film, the π_C and π_D values are increased following the exponential form of Langmuir-like growth and finally saturates when the monolayer is mostly covered by the BA molecules only. Our analysis shows that the τ value for π_C curve (τ_C) is 15.0 $\pm$ 1.2. Similarly, the τ value for π_D curve (τ_D) is 23.7 $\pm$ 1.6. To study the surface morphology and the structures of the mixed barium stearate and barium behenate films at high pH ($\approx$ 9.5) conditions, different ratios of SA and BA films in presence of Ba^{2+} ions are deposited on hydrophilic silicon Si (001) substrates in a single upstroke. Apart from the pure SA and BA films, the mixed films for different X_{SA}: X_{BA} ratios are also deposited before and after the π_C.

AFM images depicting the surface topography of the BA and SA:BA mixed films are shown in Fig. 3 (before π_C) and Fig. 4 (after π_C) respectively. The corresponding line profile is also shown in the insets of the AFM images. Fig. 3(f) represents the film of pure behenic acid, while Fig. 3(a)-(e) represents the mixed SA:BA monolayers before the collapse pressure. The pure BA films and the mixed films firmly show smooth morphology before the collapse pressure. The height profile varies from 0.6 nm to 1.5 nm. Similarly, Fig. 4(a) and 4(g) represents the film of pure stearic acid and behenic acid, while Fig. 4(b)-(f) represents the mixed SA:BA monolayer after the collapse pressure. The pure stearic acid shows collapsed film forming thick layer of multilayer structures. The maximum height obtained from the line profile is $\approx$ 20 nm. On the other hand, pure behenic acid also shows collapsed film but mostly monolayer like features is maintained except some bilayer domains on top of the monolayer. The maximum height obtained from the line profile is $\approx$ 4.9 nm. All the mixed SA:BA film shows collapsed film behaviour. The multilayer feature is observed more for the cases where the stearic acid proportion is more in the mixed film. However with the decreasing amount of stearic acid in the mixed SA:BA film the multilayer like feature also decreases. The average height of the film is obtained from the analysis of the AFM images. The values of average height for different X_{SA}: X_{BA} ratios of mixed films are 14.6 (1.0:0.0), 12.1 (0.92:0.08), 11.7 (0.83:0.17), 5.8 (0.64:0.36), 6.2 (0.44:0.56), 4.4 (0.23:0.77) and 4.6 nm (0.0:1.0) respectively.

X-ray reflectivity data (open circles) and the corresponding fits (solid lines) obtained from the BA and SA:BA mixed films before collapse (π_C) are shown in Fig. 5(a) and the corresponding EDPs obtained from the data fitting are shown in Fig. 5(b). On the other hand, X-ray reflectivity data (open circles) and the corresponding fits (solid lines) obtained from the SA, BA and SA:BA mixed films after collapse (π_C) are

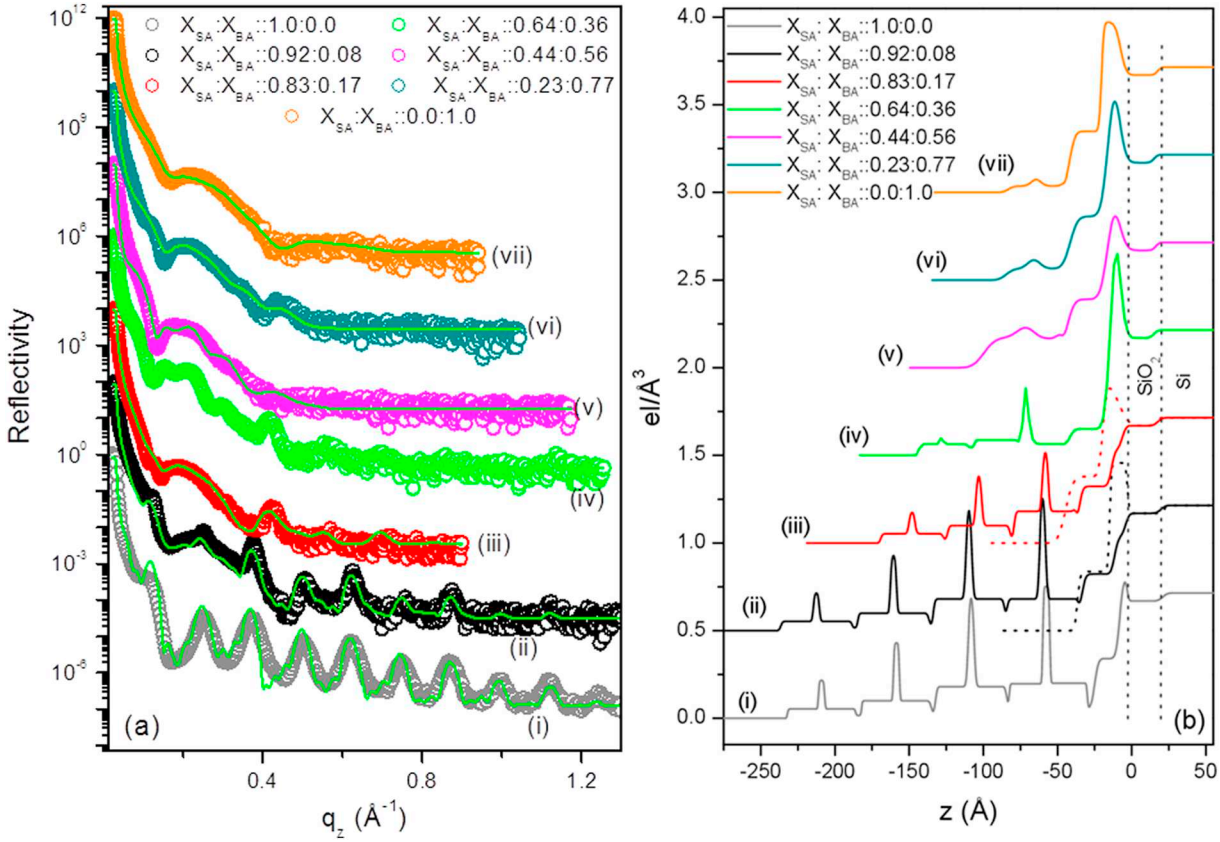

Fig. 6. (a) X-ray reflectivity data (open circles) and the respective fits (solid lines) for the films deposited after the collapse pressure (π_C) at seven different ratios of SA:BA mixed films in presence of Ba^{2+} ions at high (≈ 9.5) subphase pH condition. Reflectivity data and the corresponding fits have been vertically shifted for clarity. (b) Electron density profiles (EDPs) extracted from the fits is also shifted vertically for the same.

shown in Fig. 6(a) and the corresponding EDPs obtained from the data fitting are shown in Fig. 6(b) respectively. From the EDPs shown in Fig. 5(b) it is clear that the monolayer formed on the water surface is deposited on the silicon substrate after transfer. A higher electron density region (≈ 0.77–0.82 el/Å^3) is present near the substrate surface due to the presence of metal-bearing headgroups and a compact hydrocarbon tail region of electron density ≈ 0.29–0.35 el/Å^3 is there above such headgroup region.

However, with increasing behenic acid amount in the mixed solution, the total film thickness increases from ≈ 37 to 49 Å as the tail length of behenic acid is higher than the stearic acid. This slight increment in thickness of SA:BA mixed films with increasing amount of BA is also evidenced from the XRR profiles shown in Fig. 5(a) as the first dip in the XRR gradually shifted toward the lower q value. XRR profiles obtained from the films deposited after π_C show pseudo-Bragg peaks and in addition monolayer-like profile as shown in Fig. 6(a). The presence of Bragg peaks gradually reduced with the increase of BA amount in the mixture and for pure BA film it is negligible. As the films are transferred by the MILS method so it is expected that the structure formed by the mixed and pure fatty acids having long hydrocarbon tail is properly transferred on the solid substrate to have the actual structural information. EDPs obtained from the data fitting show that pure SA film takes multilayered structure after monolayer collapse having total four bilayers and one monolayer. Headgroups containing Ba ions show higher electron density (≈ 0.75 el/Å^3) and a bilayer spacing of ≈ 51 Å is obtained as shown in Fig. 6(b). For this film, if the hydrocarbon tail density of the substrate-attached monolayer (≈ 0.34 el/Å^3) is considered as 100%, then the coverage's of the upper layers will be ≈ 59, 53, 26 and 14% respectively toward the air side. For X_{SA}: X_{BA}:: 0.92:0.08, the XRR data is fitted by considering the combination of multilayer- and monolayer-like models having weightage of ≈ 0.5 each.

However, the coverage's of the layers above the compact monolayer toward air-side are ≈ 28, 28, 14 and 7.8% respectively. For X_{SA}: X_{BA}:: 83:0.17, the weightage of monolayer-like model is ≈ 0.75 but the weightage of the multilayer-like model is ≈ 0.25. Like before, if the coverage of the compact layer is considered as 100%, then the coverage's of the layers above the compact monolayer toward air-side are ≈ 13.2, 7.4 and 3.7% respectively. Similarly, for X_{SA}: X_{BA}:: 0.64:0.36, the coverage's of the layers above the substrate-attached monolayer are ≈ 23.5 and 17.6% respectively. However, after that trilayer-like structure is obtained as for X_{SA}: X_{BA}:: 0.44:0.56, the coverage of the upper bilayer is found as ≈ 49%, whereas for X_{SA}: X_{BA}:: 0.23:0.77 and pure behenic acid the upper bilayer coverage's are obtained as ≈ 20% and 10.5% respectively.

From the π-A isotherm of pure SA in presence of Ba^{2+} ions at high subphase pH conditions show slow rise from A = 0.30 nm^2 and continues up to A = 0.06 nm^2. Such isotherm is an indication of monolayer collapse or 2D to 3D transition at very low surface pressure. The reason behind such observation is that at high subphase pH bidentate chelate coordination forms in the metal-headgroup part of the monolayer forming molecules [39]. In the bidentate chelate and bidentate bridge conformations, the net dipole moment formed by the metal bearing headgroup lies in the perpendicular direction to the water surface [41]. Due to the presence of such out-of-plane dipole moment, the molecules prefer to move easily in the out of plane direction with barrier compression and thus the multilayer forms where bilayer-like structure is present having two molecules attached with one another through the effective out-of-plane dipole-dipole interaction of the chelate headgroups. On the other hand, π-A isotherm of pure BA in presence of Ba^{2+} ions at high subphase pH conditions shows constant pressure collapse at higher collapse pressure, i.e., at 64.6 mN/m. Thus, the hydrocarbon tail length difference for SA and BA induces two different collapse

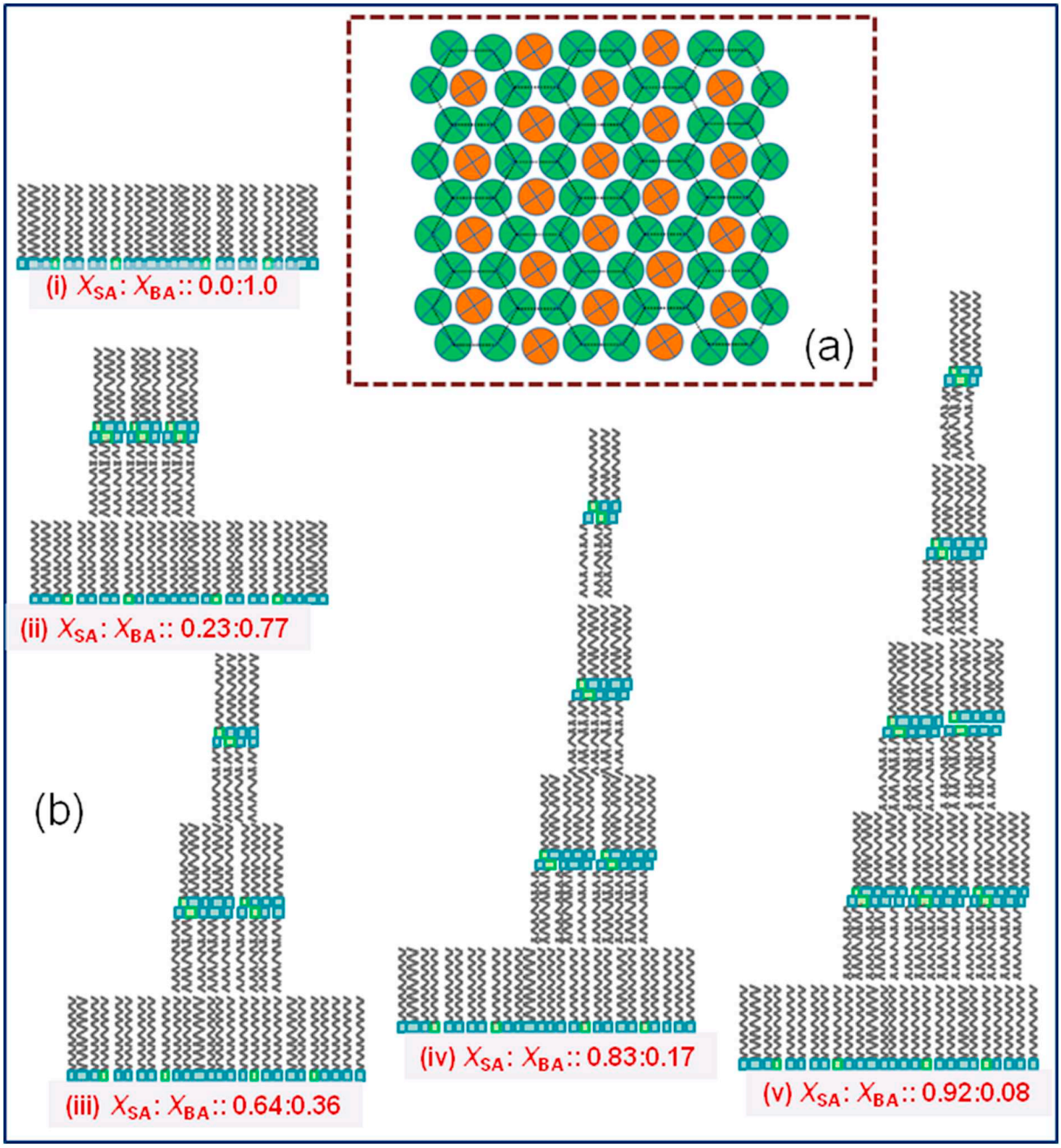

Fig. 7. (a) Probable packing structure of coexisting stearic and behenic acids molecules for a specific mixing ratio. (b) Cartoon to show the different probable collapsed structures for different SA and BA ratios: (i) X_{SA}: X_{BA}:: 0.0:1.0, (ii) X_{SA}: X_{BA}:: 0.23:0.77, (iii) X_{SA}: X_{BA}:: 0.64:0.36, (iv) X_{SA}: X_{BA}:: 0.83:0.17 and (v) X_{SA}: X_{BA}:: 0.92:0.08.

structures at higher subphase pH. The longer hydrocarbon tail length of BA molecules induces more hydrophobicity [57] and the relatively stronger tail-tail hydrocarbon interaction among these molecules hold them together on the water surface forming a connected or percolated structure as shown in Fig. 7(a) and due to this multilayer structure do not form easily under the barrier. On the other hand, due to the presence of relatively shorter tail length, SA molecules cannot produce such stronger tail-tail hydrophobic interaction and due to that it collapses easily under barrier pressure and forms multilayer structure. Thus, like headgroups, hydrocarbon tail length and the relative hydrophobicity plays a key role in determining the final structure of the films at the air-water interface [46]. However, as the ratio of BA in the SA:BA mixed film decreases the collapse nature changes from constant pressure to constant area collapse. The transition in the collapse nature occurs once the weightage of BA in the mixed film becomes less than 66%, i.e., after X_{SA}: X_{BA}:: 0.34:0.66. The change in the ratio of SA:BA mixed film not only transforms the collapse behaviour but also the π_C and π_D values and the collapsed structures. Different possible collapsed structures obtained from the analysis are shown as cartoon in Fig. 7(b). The changes in the values of π_C and π_D are such that it nearly follows the Langmuir-like growth behaviour as shown in Fig. 2. Such continuous change of π_C and π_D suggests that there is a gradual transition of materials from monolayer to multilayer state. However, this gradual transition mostly ceases when the amount of BA in the mixed film becomes more than 66%. Such very less amount of molecular transfer is also evidenced from the AFM and XRR analysis. Height profiles obtained from AFM images and EDPs obtained from the XRR analysis confirms that height or thickness of the films are minimum when BA

proportion in the SA + BA film is more than 66%. The specific value of BA amount ($\approx$ 66%) in the mixed film obtained from this study for such monolayer to multilayer collapse is comparable with the critical percolation threshold value in two-dimensional percolated networks. A percolated system has a giant connectivity that exists above a certain threshold point called as critical percolation, p_c, and it depend on the geometry of the system. Actually, in percolation theory [43,44], connected pathway exists in lattices whose bonds or sites are occupied to different extents. The bond or site percolation threshold (q_c) for a 2D lattice is the fraction (f) that needs to be randomly populated until a nearest-neighbor connected cluster spans the entire lattice. The long-range connectivity between the spanning clusters makes the system rigid with respect to applied forces. Thus, a pure BA monolayer is equivalent to a rigid and fully percolated generic 2D lattice [45], where the fraction of sites occupied is essentially unity. For mixed monolayers of BA and SA, a reduction in BA is equal to a dilution (i.e., $f < 1$) of the generic 2D lattice, where the empty bonds or sites of BA is filled up by SA. The minimum value of X_{BA} for which the mixed monolayer can have nearly the same collapse pressure as pure BA monolayer thus becomes the percolation threshold for the 2D lattice. It is known that monolayer of pure stearic acid at room temperature shows hexagonal structures [58]. In two dimensional system, for hexagonal bond percolation, $p_c = 1 - 2\sin(\pi/18) \approx 0.66$ [43–45]. The critical value obtained from our study matches well with this p_c value, which is $\approx$ 0.66 or 66%. It thus indicates that when the BA amount in the mixed film is more than 66%, the relatively stronger tail-tail hydrophobic interactions among BA molecules induces a 2D percolated network in the mixed monolayer film that holds the monolayer on the water surface and as a result negligible amount of molecular transfer takes place in the out-of-plane direction under external pressure which effectively modifies the collapse nature and collapsed structure of the mixed films.

4. Conclusions

Collapse nature of the film of mixed fatty acids, i.e., stearic and behenic acids is studied under high subphase pH ($\approx$ 9.5) condition in presence of Ba^{2+} ions. π-A curves for different ratios of SA and BA show different isotherm features. The values of collapse pressure (π_C) and dip pressure (π_D) obtained from the isotherms follow Langmuir-like growth nature, however, the pressure variation is very less at higher proportion of BA molecules in the mixed film. The monolayer is found to collapse differently for different ratios of mixed fatty acids. Monolayer shows constant pressure collapse for pure BA and the collapse nature stays nearly the same until the weightage of BA is 66% in the mixed fatty acids film. The collapse nature of the mixed film changes to constant area collapse once the critical value, i.e., 66% of BA in the mixed fatty acids system is achieved and with decrease of this value the constant area collapse continues. X-ray reflectivity and atomic force microscopy analysis shows that pure stearic acid film has multilayered structure at such pH condition. However, the multilayer feature gradually decreases with the decrease in the stearic acid ratio in the mixed film. The change in the collapse behaviour is explained considering the two-dimensional tail-tail percolated network structure formed by the BA molecules having relatively longer hydrocarbon tails.

Authors contribution

BKS and SK conceptualised the study and designed the experiments, while BKS performed all experiments. BKS and SK wrote and approved the manuscript.

Declaration of Competing Interest

The authors declare that they have no known competing financial interests or personal relationships that could have appeared to influence the work reported in this paper.

Acknowledgements

The work is supported by Department of Science and Technology (DST), India. Authors also acknowledge Council for Scientific and Industrial Research (CSIR), Govt. of India for CSIR-SRF fellowship (Grant No: 09/835(0027)/2019-EMR-I).

Appendix A. Supplementary data

Supplementary data to this article can be found online at https://doi.org/10.1016/j.colcom.2020.100261.

References

[1] V.M. Kaganer, H. Mohwald, P. Dutta, Structure and phase transitions in Langmuir monolayers, Rev. Mod. Phys. 71 (3) (1999) 779–819.
[2] H. Brockman, Lipid monolayers: why use half a membrane to characterize protein-membrane interactions? Curr. Opin. Struct. Biol. 9 (4) (1999) 438–443.
[3] T. Hianik, Structure and physical properties of biomembranes and model membranes, Acta Phys. Slovaca 56 (6) (2006) 685–805.
[4] J.R. Siqueira Jr., L. Caseli, F.N. Crespilho, V. Zucolotto, O.N. Oliveira Jr., Immobilization of biomolecules on nanostructured films for biosensing, Biosens. Bioelectron. 25 (6) (2010) 1254–1263.
[5] K. Shin, M. Rafailovich, J. Sokolov, D. Chang, J. Cox, R. Lennox, A. Eisenberg, A. Gibaud, J. Huang, S. Hsu, Observation of surface ordering of alkyl side chains in polystyrene/polyelectrolytes diblock copolymer Langmuir films, Langmuir 17 (16) (2001) 4955–4961.
[6] V. Krishnan, K. Sakakibara, T. Mori, J.P. Hill, K. Ariga, Manipulation of thin film assemblies: recent progress and novel concepts, Curr. Opin. Colloid Interface Sci. 16 (6) (2011) 459–469.
[7] R.M. Leblanc, Molecular recognition at Langmuir monolayers, Curr. Opin. Chem. Biol. 10 (6) (2006) 529–536.
[8] A. Baszkin, Molecular recognition on the supported and on the air/water interface-spread protein monolayers, Adv. Colloid Interf. Sci. 128–130 (2006) 111–120.
[9] M. Sickert, F. Rondelez, H. Stone, Single-particle Brownian dynamics for characterizing the rheology of fluid Langmuir monolayers, Eur. Phys. Lett. 79 (6) (2007) 66005–1–66005-6.
[10] P. Wydro, K. Hąc-Wydro, thermodynamic description of the interactions between lipids in ternary Langmuir monolayers: the study of cholesterol distribution in membranes, J. Phys. Chem. B 111 (10) (2007) 2495–2502.
[11] George L. Gaines Jr., Insoluble Monolayers at Liquid-Gas Interfaces, 1st ed., Interscience Publishers, New York, 1966.
[12] O. Albrecht, H. Gruler, E. Sackmann, Polymorphism of phospholipid monolayers, J. Phys. 39 (3) (1978) 301–313.
[13] D. Andelman, F. Brochard, C. Knobler, F. Rondelez, Structures and phase transitions in Langmuir Monolayers, in: A. Ben-Shaul, W.M. Gelbart, D. Roux (Eds.), Micelles, Membranes, Microemulsions, and Monolayers, 1st ed., Springer-Verlag, New York, 1994.
[14] J.H. Fendler, F.C. Meldrum, The colloid chemical approach to nanostructured materials, Adv. Mater. 7 (7) (1995) 607–632.
[15] H. Mohwald, Phospholipid Monolayers, in: R. Lipowsky, E. Sackmann (Eds.), Handbook of Biological Physics: Structure and Dynamics of Membranes, 1st ed., Vol. 1A Elsevier Science Ltd., Amsterdam, The Netherlands, 1995.
[16] K.Y.C. Lee, Collapse mechanisms of Langmuir monolayers, Annu. Rev. Phys. Chem. 59 (2008) 771–791.
[17] H.E. Ries Jr., Stable ridges in a collapsing monolayer, Nature (London) 281 (1979) 287–289.
[18] C. Ybert, W. Lu, G. Moller, C.M. Knobler, J. Phys. Chem. B 106 (8) (2002) 2004–2008.
[19] M.M. Lipp, K.Y.C. Lee, D.Y. Takamoto, J.A. Zasadzinski, A.J. Waring, Coexistence of buckled and flat monolayers, Phys. Rev. Lett. 81 (8) (1998) 1650–1653.
[20] Z. Wang, S.B. Hall, R.H. Notter, Dynamic surface activity of films of lung surfactant phospholipids, hydrophobic proteins, and neutral lipids, J. Lipid Res. 36 (6) (1995) 1283–1293.
[21] B. Robertson, H.L. Halliday, Principles of surfactant replacement, Biochim. Biophys. Acta 1408 (2–3) (1998) 346–361.
[22] D. Takamoto, M. Lipp, A. Von Nahmen, K.Y.C. Lee, A. Waring, J.A. Zasadzinski, Interaction of lung surfactant proteins with anionic phospholipids, Biophys. J. 81 (1) (2001) 153–169.
[23] A. Angelova, D. Vollhardt, R. Ionov, 2D-3D transformations of amphiphilic monolayers influenced by intermolecular interactions: a Brewster angle microscopy study, J. Phys. Chem. 100 (25) (1996) 10710–10720.
[24] C. Gourier, C.M. Knobler, J. Daillant, D. Chatenay, Collapse of monolayer of 10, 12-pentacosadiynoic acid: kinetics and structure, Langmuir 18 (2002) 9434–9440.
[25] S. Kundu, A. Datta, S. Hazra, Effect of metal ions on monolayer collapses, Langmuir 21 (13) (2005) 5894–5900.
[26] S. Kundu, A. Datta, M.K. Sanyal, J. Daillant, D. Luzet, C. Blot, B. Struth, Growth of bimolecular films of three-tailed amphiphiles, Phys. Rev. E 73 (6) (2006) 061602–1–061602-6.
[27] S. Kundu, A. Datta, S. Hazra, Growth of a collapsing Langmuir monolayer, Phys. Rev. E 73 (5) (2006) 051608–1–051608-7.

[28] S. Kundu, Collapse of preformed cobalt stearate film on water surface, Colloids Surf. A Physicochem. Eng. Aspects 348 (1–3) (2009) 196–204.
[29] M.C. Petty, Langmuir–Blodgett Films: An Introduction, Cambridge University Press, New York, 1996.
[30] E. Hatta, J. Nagao, Topological manifestations of surface-roughening collapse in Langmuir monolayers, Phys. Rev. E 67 (4) (2003) 041604–1041604-5.
[31] A. Datta, M.K. Sanyal, A. Dhanabalan, S.S. Major, Formation of highly condensed ferric stearate monolayers at the air – water Interface, J. Phys. Chem. B 101 (45) (1997) 9280–9286.
[32] D. Vollhardt, U. Retter, Nucleation in insoluble monolayers. 1. Nucleation and growth model for relaxation of metastable monolayers, J. Phys. Chem. 95 (9) (1991) 3723–3727.
[33] E. Hatta, H. Hosoi, H. Akiyama, T. Ishil, K. Mukasa, Novel pattern formation in the collapse process of floating monolayer at the air-water interface, Eur. Phys. J. B 2 (1998) 347–349.
[34] E. Hatta, Th.M. Fischer, Modulation crack growth and crack coalescence upon Langmuir monolayer collapse, J. Phys. Chem. 106 (3) (2002) 589–592.
[35] E. Le Calvez, D. Blaudez, T. Buffeteau, B. Desbat, Effect of cations on the dissociation of Arachidic acid monolayers on water studied by polarization-modulated infrared reflection – absorption spectroscopy, Langmuir 17 (3) (2001) 670–674.
[36] D. Vaknin, W. Bu, S.K. Satija, A. Travesset, Ordering by collapse: formation of bilayer and trilayer crystals by folding Langmuir monolayers, Langmuir 23 (4) (2007) 1888–1897.
[37] F. Leveiller, D. Jacquemain, M. Lahav, L. Leiserowitz, M. Deutsch, K. Kjaer, J. AlsNielsen, Crystallinity of the double layer of cadmium Arachidate films at the water surface, Science 252 (5012) (1991) 1532–1536.
[38] M. Flasinski, M. Gawry's, M. Broniatowski, P. Wydro, Studies on the interactions between parabens and lipid membrane components in monolayers at the air/aqueous solution interface, Biochim. Biophys. Acta 1858 (4) (2016) 836–844.
[39] K. Das, S. Kundu, Subphase pH induced monolayer to multilayer collapse of fatty acid salt Langmuir monolayer at lower surface pressure, Colloids Surf. A Physicochem. Eng. Asp. 492 (2016) 54–61.
[40] K. Nakamoto, Infrared and Raman Spectra of Inorganic and Coordination Compounds, Wiley, New York, 1986.
[41] S. Mukherjee, A. Dutta, Crossover from layering to island formation in Langmuir-Blodgett growth: Role of long-range intermolecular forces, Phys. Rev. E 83 (4) (2011) 041604–1041604-11.
[42] S. Mukherjee, A. Datta, Langmuir-Blodgett deposition selects carboxylate headgroup coordination, Phys. Rev. E 84 (4) (2011) 041601–1041601-7.
[43] G.R. Grimmett, Percolation, Springer-Verlag, New York, 1999.
[44] D. Stauffer, A. Aharony, Introduction to Percolation Theory, Taylor & Francis, Washington, DC, 1992.
[45] D.J. Jacobs, M.F. Thorpe, Generic rigidity percolation in two dimensions, Phys. Rev. E 53 (4) (1996) 3682–3693.
[46] A. Gopal, K.Y.C. Lee, Headgroup percolation and collapse of condensed Langmuir monolayers, J. Phys. Chem. B 110 (44) (2006) 22079–22087.
[47] A. Datta, S. Kundu, M.K. Sanyal, J. Daillant, D. Luzet, C. Blot, B. Struth, Dramatic enhancement of capillary wave fluctuations of a decorated water surface, Phys. Rev. E 71 (4) (2005) 041604–1041604-7.
[48] L.G. Parratt, Surface studies of solids by total reflection of X-rays, Phys. Rev. 95 (2) (1954) 359–369.
[49] J. Daillant, A. Gibaud, X-Ray and Neutron Reflectivity: Principles andApplications, Springer, Berlin, 1999.
[50] M. Tolan, X-Ray Scattering from Soft Matter Thin Films, Springer, Berlin, 1999.
[51] J.K. Basu, M.K. Sanyal, Ordering and growth of Langmuir–Blodgett films: X-ray scattering studies, Phys. Rep. 363 (1) (2002) 1–84.
[52] I. Horcas, R. Fernandez, J.M. Gomez-Rodrıguez, J. Colchero, J. Gomez-Herrero, A.M. Baro, WSXM: A software for scanning probe microscopy and a tool for nanotechnology, Rev. Sci. Instrum. 78 (1) (2007) 013705–1013705-8.
[53] S. Ställberg-Stenhagen, E. Stenhagen, Phase transitions in condensed monolayers of normal chain carboxylic acids, Nature 156 (1945) 239–240.
[54] G.A. Overbeck, D.D. Mobius, A new phase in the generalized phase diagram of monolayer films of long-chain fatty acids, J. Phys. Chem. 97 (30) (1993) 7999–8004.
[55] M. Durbin, A. Malik, R. Ghaskadvi, P. Zschack, P. Dutta, X-ray diffraction study of a recently identified phase transition in fatty acid Langmuir monolayers, J. Phys. Chem. 98 (7) (1994) 1753–1755.
[56] I. Ahmed, A. Haque, S. Bhattacharyya, P. Patra, J.R. Plaisier, F. Perissinotto, J.K. Bal, Vitamin C/stearic acid hybrid monolayer adsorption at air–water and air–solid interfaces, ACS Omega 11 (3) (2018) 15789–15798.
[57] F. Kampa, J.A. Hamilton, How fatty acids of different chain length enter and leave cells by free diffusion, Prostag. Leukotr. Ess. 75 (3) (2006) 149–159.
[58] K. Das, B.K. Sah, S. Kundu, Cation-induced monolayer collapse at lower surface pressure follows specific headgroup percolation, Phys. Rev. E 95 (2) (2017) 022804–1–022804-9.